

Wavelength variation of the second-order nonlinear coefficients of KNbO₃, KTiOPO₄, KTiOAsO₄, LiNbO₃, LiIO₃, β-BaB₂O₄, KH₂PO₄, and LiB₃O₅ crystals: a test of Miller wavelength scaling

William J. Alford and Arlee V. Smith

Lasers, Optics and Remote Sensing Department, Sandia National Laboratories, Albuquerque, New Mexico 87185-1423

Received July 11, 2000; revised manuscript received November 1, 2000

We measure second-order nonlinear coefficients using optical parametric amplification and second-harmonic generation over a range of wavelengths for the crystals KNbO₃, KTiOPO₄, KTiOAsO₄, LiNbO₃, LiIO₃, β-BaB₂O₄, KH₂PO₄, and LiB₃O₅. Combining our new measurements with previously reported values, we compare the wavelength variation of individual d_{ijk} 's with Miller scaling, and we conclude that Miller scaling is a useful approximation for these crystals. © 2001 Optical Society of America
OCIS codes: 190.2620, 190.4410, 190.4970.

1. INTRODUCTION

With the improving quality of lasers, nonlinear crystals, and the software tools for modeling wavelength conversion in crystals, it is increasingly important to have accurate nonlinear optical coefficients. Most second-order nonlinear coefficients have been measured by use of second-harmonic generation of 1064-nm light, but because many applications involve other wavelengths it would be useful to have a method of scaling the coefficients with wavelength. An approximation known as Miller scaling is sometimes used for this, but it is not well tested. In fact, recent measurements of several crystals over a range of wavelengths by Shoji *et al.*,¹ Boulanger *et al.*,²⁻⁴ and Zondy *et al.*⁵ cast doubt on its validity. The purpose of this paper is to more thoroughly test Miller scaling by combining our new measurements of nonlinearities with a review of previous measurements.

In a 1964 paper,⁶ Miller made the empirical observation that the quantity Δ_{ijk} , defined by

$$\Delta_{ijk} = \frac{d_{ijk}(-\omega_1 - \omega_2; \omega_1, \omega_2)}{\chi_{ii}(\omega_1 + \omega_2)\chi_{jj}(\omega_1)\chi_{kk}(\omega_2)}, \quad (1)$$

has little dispersion, varying from a constant value by only a factor of 2 or so for all noncentrosymmetric crystals and by less than 2 for individual d_{ijk} coefficients within a given symmetry class. Here d_{ijk} is the second-order nonlinear coefficient, and the χ 's are linear susceptibility tensor elements [$\chi_{ii}(\omega) = n_i^2 - 1$, where n_i is the refractive index for light of frequency ω polarized along the i axis]. Theoretical support for Miller's observation comes from calculations of the nonlinear response of a classical anharmonic oscillator^{7,8} and from various bond additivity models of simple semiconductor crystals.⁹ Both types of

calculation assume the many excited electronic states of the crystal can be treated as a single level with a transition strength proportional to a weighted sum over all the actual levels. Based on the quantum-mechanical form of the nonlinear coefficients,⁷ there is no reason to believe this should be highly accurate for most crystals. Nevertheless, for lack of a better method, a weaker form of Miller's rule, stating that a constant Δ_{ijk} is associated with each nonlinear coefficient of a particular crystal, is often invoked to extrapolate d_{ijk} 's from measured wavelengths to redder or bluer wavelengths.

We report here our measurements for the crystals potassium niobate (KNbO₃), potassium titanyl phosphate, KTiOPO₄ (KTP), potassium titanyl arsenate, KTiOAsO₄ (KTA), lithium niobate (LiNbO₃), lithium iodate (LiIO₃), beta barium borate, β-BaB₂O₄ (BBO), potassium dihydrogen phosphate, KH₂PO₄ (KDP), and lithium triborate, LiB₃O₅ (LBO). When we combine our results with previous measurements, we find the weaker form of Miller scaling, which we will call Miller scaling throughout the rest of this paper, is a reasonable approximation for all the crystals studied and is a good fit for some of them.

2. MEASUREMENT METHODS

A. Parametric Gain

We measured parametric gain using pump wavelengths of 1064 nm and 532 nm. Our 1064-nm measurements are based on parametric amplification of cw light near 1550 nm for the phase-matched process 1064 nm → ~1550 nm + ~3393 nm. We used large-diameter pump beams to minimize the effects of birefringent walk-off and measured parametric gains near the center of the pump beam to simplify analysis and improve irradiance calibra-

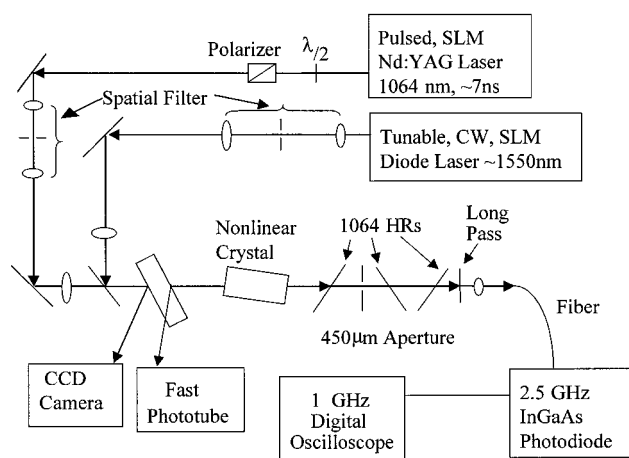


Fig. 1. Diagram of the parametric-gain experimental apparatus.

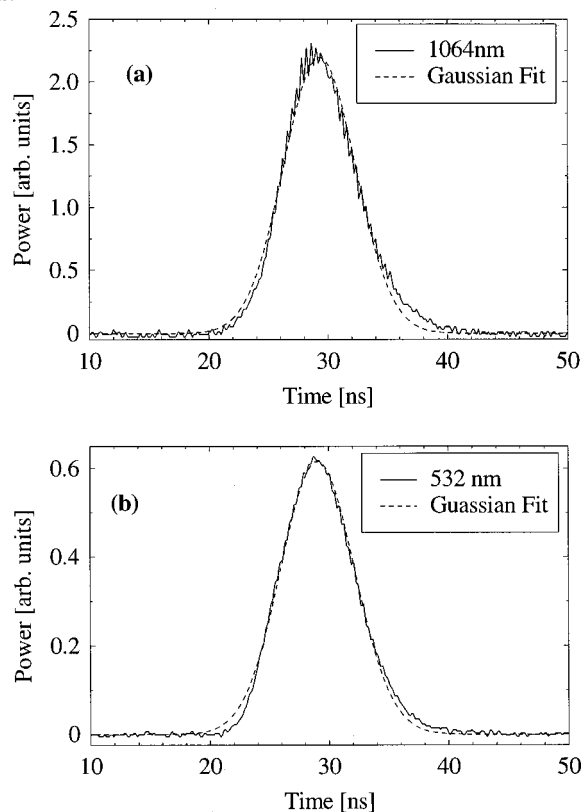


Fig. 2. Example of measured time profiles for (a) the 1064-nm and (b) the 532-nm pump pulses, with Gaussian fits.

tions. Figure 1 shows our experimental setup. An injection-seeded, Q -switched, Nd:YAG laser (Continuum NY82-10) supplies single-longitudinal-mode, 7-ns pulses at 1064 nm. We spatially filter this to provide a collimated pump beam with a near-Gaussian spatial profile of diameter 1.4 mm (FWHM irradiance) at the crystal. An external-cavity diode laser (New Focus 6200) supplies tunable, cw signal light at ~ 1550 nm that is spatially filtered and loosely focused at the nonlinear crystal to a waist of ~ 0.4 mm. The pump and signal beams parallel one another but are slightly offset to give exact spatial overlap at the crystal center. This minimizes the influence of birefringent walk-off. A 0.45-mm-diameter aperture positioned after the crystal, and laterally centered on

the 1550-nm signal beam, discriminates against stray signal light that is not centered on the pump beam. The spatial profile of the pump beam is measured by use of a video camera with beam-analysis software, positioned at an optical equivalent of the crystal input face. The fast phototube, a Hamamatsu 1328U-51, and a Tektronix 684B digital oscilloscope (1-GHz bandwidth, 2×10^9 samples/s digitizing rate), monitor the pump time profile and pulse energy on each laser pulse. This energy monitor is calibrated against an Ophir 10A-P volume-absorbing powermeter. A typical time profile for the pump pulse is shown in Fig. 2(a) along with a fit to a Gaussian profile. A fiber-coupled InGaAs photodiode (NRC AD-200, 2.5-GHz bandwidth) and a Tektronix 684B oscilloscope record the 1550-nm signal irradiance. From this we determine the magnitude of the parametric gain at the peak of the pump pulse. Typical gains, defined as the signal maximum at the peak of the pump power divided by the cw signal, range from 2 to 20. Figure 3 shows example gain signals for low gain in Fig. 3(a) and high gain in Fig. 3(b). Three 1064-nm high-reflectivity mirrors plus a 1400-nm long-pass filter placed between the nonlinear crystal and the detector ensure that the pump light alone produces no signal in the detector. For the 532-nm pumped measurements we place a KTP frequency-doubling crystal in the 1064-nm beam upstream of the spatial filter. The 532-nm pumped measurements are based on the phase-matched parametric gain process $532 \text{ nm} \rightarrow \sim 1550 \text{ nm} + \sim 810 \text{ nm}$. Figure 2(b) shows a typical 532-nm time profile and its Gaussian fit.

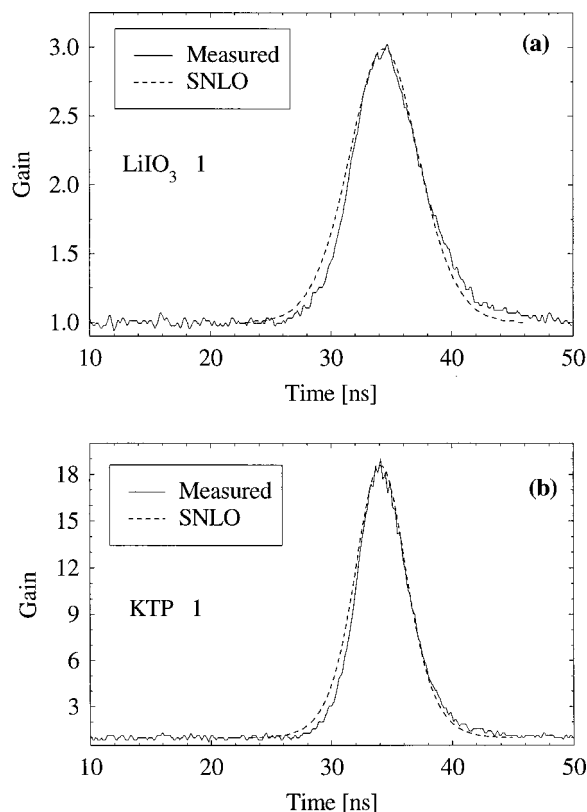


Fig. 3. Example of measured gain profiles for (a) 1064-nm-pumped LiIO_3 crystal 1 and (b) 1064-nm-pumped KTP crystal 1. The curves labeled SNLO are computed curves from the best-fit nonlinear coefficients.¹¹

This method of measuring nonlinearities has the advantage that the signal detector need not be absolutely calibrated because we measure only the gain. It is sufficient to demonstrate a fast time response and linearity. Additionally, the parametric gain for phase-matched plane-wave mixing is given in SI units by

$$\text{Gain} = \cosh^2(\gamma L_{\text{crystal}}), \quad (2)$$

where

$$\gamma = \left(\frac{2d_{\text{eff}}^2 I_p \omega_s \omega_i}{n_s n_i n_p c^3 \epsilon_0} \right)^{1/2} \quad (3)$$

and I_p is the pump irradiance. This relationship between measured gain and d_{eff} means that measurement errors in pump irradiance and gain introduce relatively little error in the deduced value of d_{eff} . In contrast, for second-harmonic generation the second-harmonic signal is proportional to the product ($d_{\text{eff}}^2 L_{\text{crystal}}^2 I_{\text{pump}}^2$) so the influence of irradiance measurement error is relatively large. Further, if the crystal is tilted slightly so there is little overlap between the primary signal beam and the signal beam after it reflects off the output and then the input face, the reflections of the signal wave at the crystal faces are unimportant, unlike Maker-fringe measurements.

Our InGaAs detector satisfies the speed and linearity requirement. The fiber coupling also avoids the problem of overfilling the small active area typical of fast semiconductor detectors. We found this was a problem with similar lens-coupled solid-state detectors. We discovered this by comparing gains measured by the fiber-coupled detector with those from two separate lens-coupled detectors (New Focus 1611 and Electro-Optics Technology 3000) with similar detector designs. The lens-coupled detectors gave lower apparent peak gains than the fiber-coupled detector did. We believe this is because some of the light strikes the InGaAs material surrounding the fast-responding InGaAs active region. The surrounding material has equal sensitivity but a slower response time. Previous measurements¹⁰ with the lens-coupled New Focus 1611 detector probably suffered from this overfilling problem, so the d_{eff} 's we reported there were probably slightly lower than their true values.

To ensure accuracy in our measurements, it is important to show that the crystals are of high quality, with no inhomogeneities such as refractive-index variations or ferroelectric domains like those found in earlier KTP measurements.¹⁰ We tested crystal quality by measuring the acceptance bandwidths and comparing them with expectations based on established Sellmeier equations. Figure 4 shows an example measurement for KTP. All the crystals reported in this paper show good agreement between the measured and calculated acceptance bandwidths. It is also necessary to ensure zero phase-velocity mismatch in our measurements. Critically phase-matched crystals (LiNbO_3 , KNbO_3 , LiIO_3 , and KTP with 532-nm pumping) were mounted on a rotation stage with an angular resolution of 0.05 mrad, much less than the smallest angular tolerance of these crystals (0.37 mrad for LiIO_3), and the angle was adjusted to maximize the gain. Two noncritically phase-matched crystals, KTA

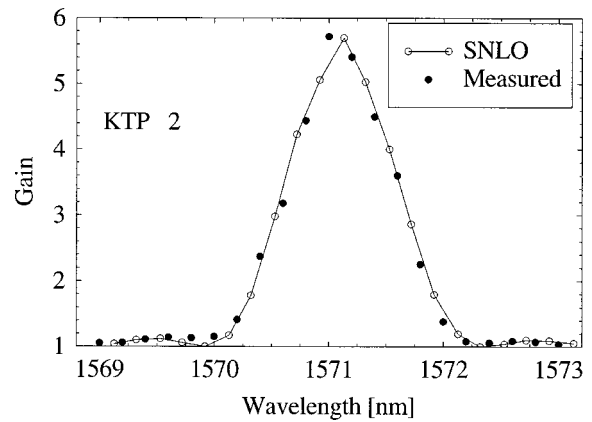


Fig. 4. Example phase-matching curve for 1064-nm-pumped KTP crystal 2. The curve labeled SNLO is a computed¹¹ phase-matching curve with Δk 's based on the KTP Sellmeier equation of Vanherzeele *et al.*¹²

and KTP with 1064-nm pumping, were phase matched at room temperature by tuning the external-cavity diode laser for maximum gain. This laser has a tuning resolution of 0.02 nm, much better than typical acceptance bandwidths of ~ 1 nm. The noncritically phase-matched LBO crystal was temperature tuned to obtain phase matching at ~ 120 °C with a temperature resolution of 0.1 °C, much better than its temperature bandwidth of 2.8 °C.

We used a detailed numeric computer model of parametric mixing, function 2D-mix-LP in the SNLO nonlinear optics code,¹¹ to find the value of d_{eff} that best matched our measurement. This model assumes Gaussian spatial and temporal profiles and includes diffraction, birefringence, and linear absorption. Measured spatial and temporal widths are used in the model. The assumption of a Gaussian time profile is a slight approximation because the rising edge of our laser pulse is slightly faster than the falling edge, as can be seen in Fig. 3. Birefringent walk-off significantly affects some of the cases, but it is accounted for in the model. Linear absorption is assumed negligible for all cases except for the KTP pumped by 1064-nm light. A spectrophotometer measurement of our KTP crystal indicates it has an absorption coefficient of 0.065/mm for the 3288-nm idler wavelength. Other input parameters for the model include wavelengths, indices of refraction, pump energy, pump pulse duration and beam diameter, crystal length, phase mismatch (assumed zero for d_{eff} determination), and d_{eff} . All the input parameters are either measured or calculated from index-of-refraction data except for d_{eff} , which we adjust to match the experimental peak gain. Typical fits of calculation to measurement are shown in Fig. 3.

All the crystals, except LBO, are antireflection coated for the pump wavelength, with identical coatings on the two end faces. Nonetheless, we measured pump transmission through the crystals at nonnormal incidence (to avoid interference effects) and determined the transmission at each surface, assuming this to be the only contributor to the transmission loss. Typical measured surface transmissions fell in the range 95–99.5%, and this correction to the measured incident pump energy was used in the computer model. Reflectivity at the signal

wavelength is unimportant because it affects the cw and amplified light to the same extent.

The precision of our d_{eff} measurements is limited primarily by uncertainties in the measured peak gain, crystal length, and pump irradiance. We estimate the experimental uncertainty in the gain measurements and the crystal lengths to be 4–5%. The uncertainty in the pump irradiance is 10%. Combined, these give an overall uncertainty in d_{eff} of 8%.

B. Second-Harmonic Generation

We measured d_{eff} 's for frequency doubling of 806-nm light in LiIO_3 , 980-nm light in KNbO_3 , 1064-nm light in KDP and BBO, and 1319-nm light in KNbO_3 , BBO, KDP, LiIO_3 , LiNbO_3 , and KTP. The 806-nm light was from an external-cavity semiconductor laser coupled to a tapered waveguide amplifier. The external-cavity laser consisted of an SDL 5412 single-mode diode laser, a collimating lens, and an 1800-lines/mm holographic grating used in a Littrow configuration. The waveguide amplifier was an SDL 8630 diode laser modified to act as a single-pass amplifier. We spatially filtered the beam and focused it into the LiIO_3 crystal, adjusting the confocal parameter, waist location, and crystal angle to maximize the 403-nm second-harmonic power.

The 980-nm source laser was a vertical, external-cavity, surface-emitting laser (VECSEL) made of a semiconductor Bragg stack rear reflector, a quantum-well

gain region similar to that described by Raymond *et al.*,¹³ and a dielectric front mirror. The front mirror has a reflectivity of 97% and a 25-mm radius of curvature. It is placed ~ 24 mm from the semiconductor wafer. Two 100- μm -thick intercavity etalons are used. One, near normal incidence, forces single-longitudinal-mode operation, the other at Brewster's angle stabilizes the polarization. We optically pump the VECSEL with a cw, Ti:sapphire laser (Coherent 899). The 980-nm VECSEL output power was 120 mW in a lowest-order Gaussian transverse mode.

The 1319-nm and 1064-nm sources were cw, single-frequency, Nd:YAG lasers (Lightwave models 126-1319-250 and 122-1064-200) with TEM00 output beams. Although the beams were TEM00, we found it necessary to insert a weak ($f = 40$ cm) cylindrical lens to correct slight astigmatism. For type I doubling we adjusted the confocal parameter, waist location, and crystal angle to maximize the second-harmonic power. For type II doubling we did the same but also measured the far-field divergence to infer the focal size in the crystal.

For the second-harmonic measurements we measured fundamental and second-harmonic powers absolutely. For the fundamental we used a volume-absorbing powermeter (Ophir 10A-P), for the harmonic a photodiode powermeter (Ophir PD-300 or PD-300-UV). The experimentally optimized focusing conditions for type I doubling were assumed to be those given by Boyd and Kleinman,¹⁴ so we based our derivation of d_{eff} on their analysis. For

Table 1. Summary of d_{eff} and d_{ijk} Measurements

Crystal	$\lambda_{\text{polarization}}[\text{nm}]$	Phase-Match Angle (θ, ϕ)	Expression ^a for d_{eff}	Measured d_{eff} [pm/V]	Deduced d_{ijk} [pm/V]
KDP	$532_e \rightarrow 1064_o + 1064_o$	$41.1^\circ, -45^\circ$	$d_{zxy}C_\theta$	0.270	$d_{zxy} = 0.398$
KDP	$660_e \rightarrow 1319_o + 1319_o$	$44.8^\circ, -45^\circ$	$d_{zxy}C_\theta$	0.227	$d_{zxy} = 0.314$
KTP 3	$532_o \rightarrow 1550_o + 810_e$	$59^\circ, 0^\circ$	$d_{yyz}S_\theta$	3.44	$d_{yyz} = 3.90$
KTP 4	$532_o \rightarrow 1550_o + 810_e$	$59^\circ, 0^\circ$	$d_{yyz}S_\theta$	3.40	$d_{yyz} = 3.86$
KTP 3	$660_o \leftarrow 1319_o + 1319_e$	$59.8^\circ, 0^\circ$	$d_{yyz}S_\theta$	3.01	$d_{yyz} = 3.40$
KTP 1	$1064_y \rightarrow 1572_y + 3288_z$	$90^\circ, 0^\circ$	d_{yyz}	2.81	$d_{yyz} = 2.81$
KTP 2	$1064_y \rightarrow 1572_y + 3288_z$	$90^\circ, 0^\circ$	d_{yyz}	2.95	$d_{yyz} = 2.95$
KTA 1	$1064_y \rightarrow 1535_y + 3468_z$	$90^\circ, 0^\circ$	d_{yyz}	2.90	$d_{yyz} = 2.90$
KTA 2	$1064_y \rightarrow 1535_y + 3468_z$	$90^\circ, 0^\circ$	d_{yyz}	2.92	$d_{yyz} = 2.92$
KNbO_3 2	$491_e \rightarrow 982_o + 982_o$	$0^\circ, 0^\circ$	$d_{xyy}C_\theta$	8.62	$d_{xyy} = 8.62$
KNbO_3 1	$660_e \rightarrow 1319_o + 1319_o$	$33^\circ, 0^\circ$	$d_{xyy}C_\theta$	5.00	$d_{xyy} = 6.23$
KNbO_3 1	$1064_e \rightarrow 1550_o + 3393_o$	$42^\circ, 0^\circ$	$d_{xyy}C_\theta$	4.42	$d_{xyy} = 6.31$
LiIO_3 3	$403_e \leftarrow 806_o + 806_o$	$42^\circ, \text{any}$	$d_{zxx}S_\theta$	3.83	$d_{zxx} = 5.23$
LiIO_3 2	$660_e \rightarrow 1319_o + 1319_o$	$24.3^\circ, \text{any}$	$d_{zxx}S_\theta$	1.83	$d_{zxx} = 3.90$
LiIO_3 1	$1064_e \rightarrow 1550_o + 3393_o$	$19.5^\circ, \text{any}$	$d_{zxx}S_\theta$	1.55	$d_{zxx} = 4.05$
LiIO_3 2	$1064_e \rightarrow 1550_o + 3393_o$	$19.5^\circ, \text{any}$	$d_{zxx}S_\theta$	1.58	$d_{zxx} = 4.13$
LiNbO_3 3	$660_e \rightarrow 1319_o + 1319_o$	$57.9^\circ, 30^\circ$	$d_{zxx}S_\theta - d_{yyy}C_\theta S_{3\phi}$	4.05	$d_{zxx} = 3.77^b$
LiNbO_3 1	$1064_e \rightarrow 1550_o + 3393_o$	$47^\circ, 30^\circ$	$d_{zxx}S_\theta - d_{yyy}C_\theta S_{3\phi}$	3.72	$d_{zxx} = 3.46^b$
LiNbO_3 2	$1064_e \rightarrow 1550_o + 3393_o$	$47^\circ, 30^\circ$	$d_{zxx}S_\theta - d_{yyy}C_\theta S_{3\phi}$	3.79	$d_{zxx} = 3.52^b$
BBO 1	$532_e \rightarrow 1550_o + 810_o$	$22.1^\circ, -30^\circ$	$d_{zxx}S_\theta - d_{yyy}C_\theta S_{3\phi}$	2.00	$d_{yyy} = 2.19^c$
BBO 2	$532_e \leftarrow 1550_o + 810_o$	$22.1^\circ, -30^\circ$	$d_{zxx}S_\theta - d_{yyy}C_\theta S_{3\phi}$	2.08	$d_{yyy} = 2.28^c$
BBO 1	$532_e \leftarrow 1064_o + 1064_o$	$22.8^\circ, -30^\circ$	$d_{zxx}S_\theta - d_{yyy}C_\theta S_{3\phi}$	2.03	$d_{yyy} = 2.24^c$
BBO 1	$660_e \leftarrow 1319_o + 1319_o$	$20.4^\circ, -30^\circ$	$d_{zxx}S_\theta - d_{yyy}C_\theta S_{3\phi}$	1.73	$d_{yyy} = 1.87^c$
BBO 2	$660_e \leftarrow 1319_o + 1319_o$	$20.4^\circ, -30^\circ$	$d_{zxx}S_\theta - d_{yyy}C_\theta S_{3\phi}$	1.77	$d_{yyy} = 1.91^c$
LBO	$532_y \rightarrow 1550_z + 810_z$	$90^\circ, 0^\circ$	d_{yzz}	1.04	$d_{yzz} = 1.04$

^a $S_{3\phi} = \sin(3\phi)$; $S_\theta = \sin(\theta + \rho)$; $C_\theta = \cos(\theta + \rho)$, where ρ is the walk-off angle.

^bAssuming $d_{yyy}/d_{zxx} = -0.49$.

^cAssuming $d_{yyy}/d_{zxx} = 55$.

type II doubling we used the inferred waist size and SNLO modeling to find d_{eff} . We also used SNLO modeling to fit the type I KDP data because it slightly absorbs the fundamental wavelengths. We measured absorption coefficients at 1319 nm and 1064 nm of 0.033/mm and 0.0072/mm, respectively.

3. RESULTS

In this paper we compare nonlinear coefficients according to the bluest of the three interacting wavelengths. It remains to be determined how the coefficients vary with changes in the two longer wavelengths. For example, we do not know how d_{ijk} for 1064 nm \rightarrow 2128 nm + 2128 nm compares with that for 1064 nm \rightarrow 1535 nm + 3468 nm. However, it seems likely the coefficients differ relatively little because the detunings of the two redder wavelengths from the degenerate wavelength of 2128 nm are in opposite directions and so probably influence the nonlinearity in opposite directions. Change in the bluest wavelength, in contrast, shifts all three wavelengths to the blue. With this justification we plot all nonlinearities against the bluest wavelength of the mixing process and assume the tuning of the redder wavelengths is relatively unimportant. Our measurements are summarized in Table 1.

One source of confusion in comparing d_{ijk} 's for biaxial crystals is the use of various axis systems. In this paper we use only the axis convention in which $n_x < n_y < n_z$ for the biaxial crystals (KTA, KTP, KNbO₃, and LBO). Angle θ is measured from the z axis, and ϕ is measured from the x - z plane toward the y - z plane. This convention means our notation will differ from some papers in the literature. This is especially true for KNbO₃, where several axis systems have been used.

Another issue is whether Kleinman symmetry has been assumed in deriving the nonlinear coefficients. This approximate symmetry states that the polarizations can be permuted independent of the frequencies without changing the value of the coefficient. For example, $d_{ijk}(-\omega_p; \omega_s, \omega_i) = d_{jik}(-\omega_p; \omega_s, \omega_i)$. This is a good approximation in the limit that all wavelengths are far from any resonances, and it has usually been found to hold within experimental accuracy except in a few cases such as KTP¹ and LiIO₃.¹⁵ It is not necessary to invoke this approximation in any of the measurements reported here, and thus our results are not based on an assumption of Kleinman symmetry.

A. KDP

KDP has been thoroughly studied for 1064-nm doubling over the past 30 years, and its d_{zxy} (d_{36}) coefficient has become the best standard for comparing second-order nonlinearities. Somewhat surprisingly though, very few data at other wavelengths are available. Our KDP crystal was purchased in 1980 from Isomet. We used frequency doubling of 1319-nm and 1064-nm light to deduce d_{eff} 's of 0.227 pm/V at 660 nm and 0.270 pm/V at 532 nm. These translate to d_{zxy} 's of 0.314 pm/V and 0.398 pm/V, which we plot in Fig. 5. Our 532-nm value of 0.398 pm/V

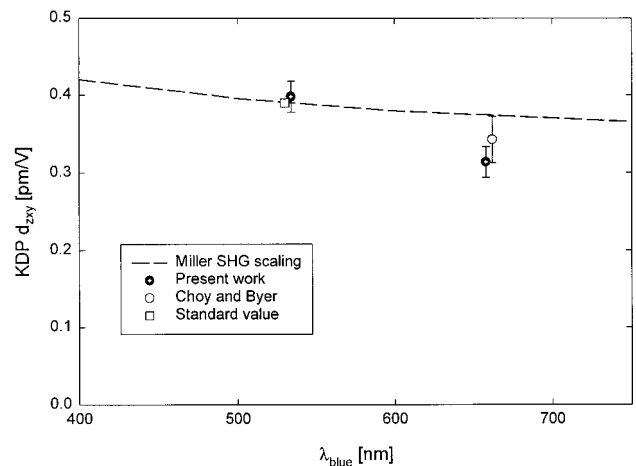


Fig. 5. KDP d_{zxy} value deduced from Choy's and Byer's¹⁷ ratio $d_{zxy}(\text{KDP})/d_{zxx}(\text{LiIO}_3) = 0.088 \pm 0.01$ for 1319-nm frequency doubling. We use our measured value of $d_{zxx}(\text{LiIO}_3) = 3.90$ pm/V. The dashed curve is Miller scaling normalized to the standard value of $d_{zxy} = 0.39$ pm/V for 1064-nm frequency doubling. The points at 532 nm and 660 nm have been plotted with small wavelength offsets for clarity.

agrees well with the accepted standard of 0.39 pm/V.¹⁶ The point labeled Choy and Byer¹⁷ is derived with their reported value of 0.088 ± 0.01 for the ratio $d_{zxy}(\text{KDP})/d_{zxx}(\text{LiIO}_3)$ for 1319-nm second-harmonic generation, combined with our measured value of 3.90 pm/V for d_{zxx} for LiIO₃ for the same process. The resulting value agrees well with ours. The dashed curve shows the Miller scaling curve for second-harmonic generation normalized to the standard value at 532 nm. Comparing the measured values with the Miller curve, we conclude that d_{zxy} may decrease slightly faster than Miller scaling with increasing wavelength, but more data are needed for a firm conclusion.

B. KTP

We characterized KTP using 1064-nm and 532-nm pumped parametric-gain measurements and by frequency doubling 1319-nm light. In the 1064-nm pumped gain measurements we characterized two flux-grown, x -cut KTP crystals for 1064_y nm \rightarrow 1572_y nm + 3288_z nm. Here the subscripts indicate the polarization direction for each wavelength. We found the two crystals agreed well and gave $d_{yyz} = 2.88 \pm 0.2$ pm/V. Figure 6 shows this value along with a dashed curve corresponding to second-harmonic Miller scaling, normalized to the 532-nm point. If we were to apply a Miller correction to our point at 1064 nm to account for the inequality of the signal and idler wavelengths, it would increase by 2.5%, agreeing slightly better with the Miller curve.

For the 532-nm-pumped gain measurements we characterized two flux-grown crystals cut for propagation at 51° from the z axis in the x - z plane. Both crystals (KTP 3 and KTP 4) were purchased from Philips Components. Tilting the crystal $\sim 8^\circ$ phase matches 532_o nm \rightarrow 1550_o nm + 810_e nm. The expression for d_{eff} in the x - z plane is $d_{\text{eff}} = d_{yyz} \sin(\theta + \rho)$, where θ is measured from the z axis and ρ is the walk-off angle. Again the two

crystals agreed, with an average of $d_{\text{eff}} = 3.42 \pm 0.3$ pm/V, implying $d_{yyz} = 3.88 \pm 0.3$ pm/V. Our earlier measurement¹⁰ was also based on a phase-matched parametric-gain measurement of 532_o nm \rightarrow 800_e nm + 1588_o nm. However, the value we reported, $d_{yyz} = 3.4$ pm/V, was smaller than the 3.88 pm/V reported here, owing to the detector overfilling effect described above in Subsection 2.A.

Our 1319-nm second-harmonic measurements used the same crystals as the 532-nm-pumped gain measurements. Note that this measurement is phase matched in the x - z plane rather than the x - y plane commonly used for 1064-nm doubling.

Several previous measurements by other authors are also included in Fig. 6. That of Anema and Rasing¹⁸ was based on Maker-fringe measurements of 1064-nm doubling. They report $d_{yyz} = 3.37$ pm/V with no error estimate. Those of Boulanger *et al.*²⁻⁴ are based on phase-matched second-harmonic generation of 1320-nm and 1064-nm light in spherical and parallelepiped KTP samples. For 1320-nm doubling they find $d_{yyz} = 2.42 \pm 0.24$ pm/V and for 1064-nm doubling $d_{yyz} = 2.65 \pm 0.13$ pm/V. Cheung *et al.*¹⁹ used parametric fluorescence from 527_o nm \rightarrow 900_e nm + 1269_o nm in a 5-mm-long, $\theta=69^\circ$, $\phi=0^\circ$ crystal to find $d_{yyz} = 4.1 \pm 0.4$ pm/V. Their pump light was a train of 8-ps pulses. Nishikawa and Uesugi²⁰ studied the parametric generation process 600_o nm \rightarrow 1200_o nm + 1200_e nm in a 5-mm-long, $\theta = 67.3^\circ$, $\phi = 0^\circ$ crystal to deduce $d_{yyz} = 4.2 \pm 0.2$ pm/V. Their pump light was a train of 1.2-ps pulses. Shoji *et al.*¹ used cw second-harmonic Maker-fringe measurements in an x -cut sample for fundamental wavelengths of 1313, 1064, and 852 nm. Their fundamental light was polarized at 45° to the y and z axes, and the second harmonic was y polarized, so these are direct measurements of coefficient d_{yyz} . Note that they use a reference frame with x and y reversed relative to ours, so their d_{15} corresponds to our d_{yyz} . Their values are $2.6 \pm$

0.13 pm/V at 1313 nm, 3.7 ± 0.2 pm/V at 1064 nm, and 3.9 ± 0.2 at 852 nm. They also measured d_{zyy} at 1064 nm, obtaining a value of 3.7 ± 0.2 pm/V demonstrating that, for this case, $d_{yyz} = d_{zyy}$, satisfying Kleinman symmetry within the experimental uncertainty. Vanherzeele and Bierlein²¹ used Maker-fringe second-harmonic generation to measure d_{yyz} in KTP relative to d_{xxx} in crystalline quartz. Their 880-nm light was a train of 5–50-ps pulses. They derived a value of 3.92 ± 0.4 pm/V by using Miller's rule to correct for dispersion of quartz from 1064 nm to 880 nm. Zondy *et al.*⁵ deduced d 's from phase-matched second-harmonic generation of 1300-nm and 2532-nm light. Both of their measurements were based on type II phase matching for propagation in the x - z plane with the fundamental polarized equally in the o and e directions and the harmonic polarized in the o direction. They report values for d_{yyz} of 2.3 ± 0.2 pm/V at 2532 nm and 2.45 ± 0.2 pm/V at 1300 nm.

The data summarized in Fig. 6 beg for discussion and explanation. We believe the 532-nm points solidly establish a value close to our 3.88 ± 0.3 pm/V. The bluer data of Vanherzeele and Bierlein²¹ and Shoji *et al.*¹ are consistent with Miller scaling from this value, albeit at the limits of the measurement error. What stands out is the strong departure from the Miller curve of the cluster of points near 650 nm and the point at 1265 nm, which all fall well below the Miller curve. This is in contrast to our points at 660 nm and 1064 nm, which lie close to the Miller curve. It seems unlikely that the actual curve would have such a structured wavelength dependence. While we cannot say that the points below the curve are incorrect, we can point out some plausible explanations. First, we note that Boulanger's measurements used multi-longitudinal-mode cw lasers. To account for this, they apply a correction of $(N/2N - 1)^{1/2}$ to their measured d , where N is the number of longitudinal modes. This correction is appropriate for N simultaneously operating modes with random phase. However, most homogeneously broadened cw lasers rapidly hop from mode to mode with only a single or a very few modes active simultaneously. In the limit of one mode oscillating at a time, the factor should be unity rather than 0.72. This would increase their value of d by 1.4, bringing both the 532-nm and the 650-nm values of Boulanger *et al.* quite close to the plotted Miller curve. We point out that Boulanger *et al.*'s measurements also give similarly low values for the other members of the KTP family compared with other measurements. Shoji *et al.*'s 532-nm values for each of the several crystals measured are in excellent agreement with the consensus values. However, their 656-nm points for KTP, BBO, and LiNbO₃ fall well below the Miller curves. This suggests the possibility of a systematic error in their measurements at this particular wavelength. The two data points of Zondy *et al.* bracket ours in wavelength but lie well below the Miller curve. We have verified their analysis based on their reported input and output powers and beam diameters, and we can offer no explanation other than possible miscalibration of input or output power or beam size.

We summarize our assessment of the wavelength variation of d_{yyz} for KTP by noting that significant discrepancies exist in the data, but we believe that a major-

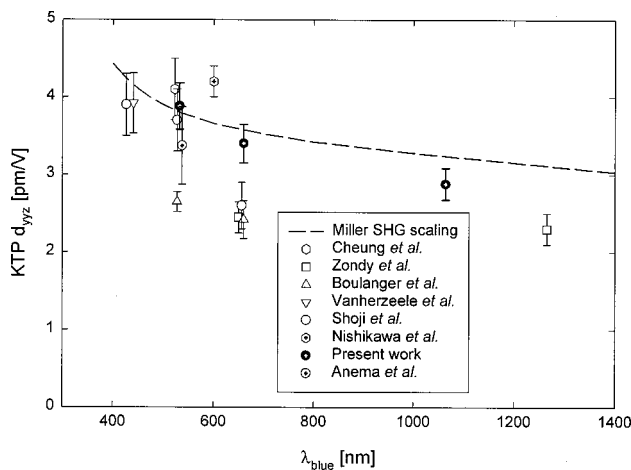


Fig. 6. KTP d_{yyz} values measured by Cheung *et al.*,¹⁹ Zondy *et al.*,⁵ Boulanger *et al.*,²⁻⁴ Vanherzeele and Bierlein,²¹ Shoji *et al.*,¹ Nishikawa and Uesugi,²⁰ Anema and Rasing,¹⁸ and in the present research. The dashed curve is Miller scaling for second-harmonic generation, normalized to the best-estimate 532-nm point. The points at 532 nm have been plotted with small wavelength offsets for clarity.

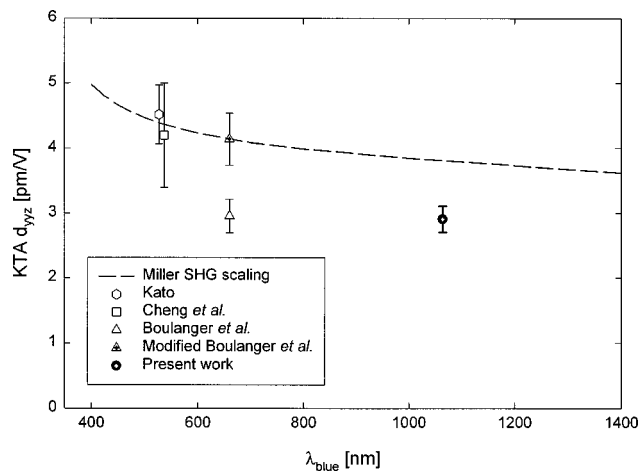


Fig. 7. KTA d_{yyz} values measured by Kato,²³ Cheng *et al.*,²² Boulanger *et al.*,^{2,24} and in the present research. The dashed curve is Miller scaling for second-harmonic generation, normalized to the best-estimate 532-nm point. The point labeled modified Boulanger is that of Boulanger multiplied by 1.4 (see text for explanation).

ity of the data indicate that Miller scaling is indeed a good approximation.

C. KTA

We measured d_{yyz} in two x -cut, 10-mm-long, flux-grown KTA crystals from Crystal Associates, using the parametric-gain process 1064_y nm \rightarrow 1535_y nm + 3468_z nm. Our d_{yyz} values are 2.90 and 2.92 for the two crystals. As shown in Fig. 7, there are three previous measurements of this coefficient^{2,22,23} at shorter wavelengths. Note that Boulanger *et al.*² find that d_{yyz} for KTA is 1.25 times that of KTP for doubling 1319-nm light. So we also plot their KTA value as 1.25 times their modified KTP value, the modification being our removal of their mode-correction factor of 0.72. Although Boulanger *et al.* find d_{yyz} for KTA is 1.25 times larger than for KTP at 660 nm, we find at 1064 nm that it is 1.3 times smaller. So although Miller scaling was a good approximation for KTP, it is less accurate for KTA, based on the sparse available data.

D. KNbO₃

We measured d_{xyy} for two KNbO₃ crystals. Crystal 1 was a critically phase-matched KNbO₃ crystal from Virgo cut for propagation in the x - z plane at $\theta=41^\circ$. Tilting this crystal 1° phase matches 1064_e nm \rightarrow 1550_o nm + 3393_o nm. The effective nonlinear coefficient is given by $d_{\text{eff}} = d_{xyy} \cos(\theta + \rho)$. We measure $d_{\text{eff}} = 4.42$ pm/V, implying $d_{xyy} = 6.31$ pm/V. We also use this crystal for frequency doubling 1319 nm by tilting it 8° . This measurement gave a $d_{\text{eff}} = 5.00$ pm/V, implying $d_{xyy} = 6.23$ pm/V.

Crystal 2, from VLOC, was cut perpendicular to the z axis (b axis) for frequency doubling 982-nm light. It is antireflection coated for 980 nm and is used at near-normal incidence. The second-harmonic power with optimum focusing indicates $d_{xyy} = 8.62$ pm/V.

Our three values are plotted in Fig. 8 along with a Miller curve that fits our values well. We also show mea-

surements from Uematsu²⁴ and Baumert *et al.*²⁵ Both these measurements are reported relative to d_{11} of quartz. To translate these to absolute values, we use $d_{11} = 0.30$ pm/V for 1064-nm doubling^{1,16} and $d_{11} = 0.31$ pm/V for 825-nm doubling (Miller scaling the 1064-nm value). Our measured nonlinearities are clearly lower than the previous measurements and may explain why some KNbO₃ optical parametric oscillators have higher-than-expected pump thresholds.²⁶

E. LiIO₃

We characterized two 30-mm-long LiIO₃ crystals cut at 22° . This allowed phase matching 1064_e nm \rightarrow 1550_o nm + 3393_o nm at $\theta = 19.5^\circ$. The two crystals agree well and give an average $d_{\text{eff}} = 1.57$ pm/V. Using $d_{\text{eff}} = d_{zxx} \sin(\theta + \rho)$, we find $d_{zxx} = 4.09$ pm/V. We also used one of these crystals to frequency double 1319 nm. The measured second-harmonic power gave $d_{\text{eff}} = 1.83$ pm/V, implying $d_{zxx} = 3.90$ pm/V.

We also characterized a 10-mm-long crystal cut at 42° by doubling 557 mW of 806-nm light to produce $64.1 \mu\text{W}$ at 403 nm. According to a Boyd and Kleinman¹⁴ analysis, this implies $d_{\text{eff}} = 3.83$ pm/V, within 1% of the value derived by numerically modeling¹¹ this process. This corresponds to $d_{zxx} = 5.23 \pm 0.52$ pm/V. The uncertainty in this measurement is mainly due to uncertainty in the measured power at 403 nm.

Previous measurements include Eckardt *et al.*'s²⁷ phase-matched doubling of 1064-nm light giving $d_{zxx} = 4.1 \pm 0.4$ pm/V,⁹ a measurement¹⁵ based on separated-beam, nonphase-matched doubling of 1064-nm light, giving $d_{zxx} = 4.36 \pm 0.3$ pm/V, and cw parametric fluorescence measurements by Borsa *et al.*²⁸ at pump wavelengths of 351, 458, 477, and 488 nm. These are shown in Fig. 9 along with a Miller-scaling curve normalized to our 532-nm point. It is evident that Miller scaling agrees with the measurements for LiIO₃.

F. LiNbO₃

We measured two 10-mm-long, congruent LiNbO₃ crystals from Castech. Both were cut for type I phase matching of 1064_e nm \rightarrow 1550_o nm + 3393_o nm at $\theta = 47^\circ$,

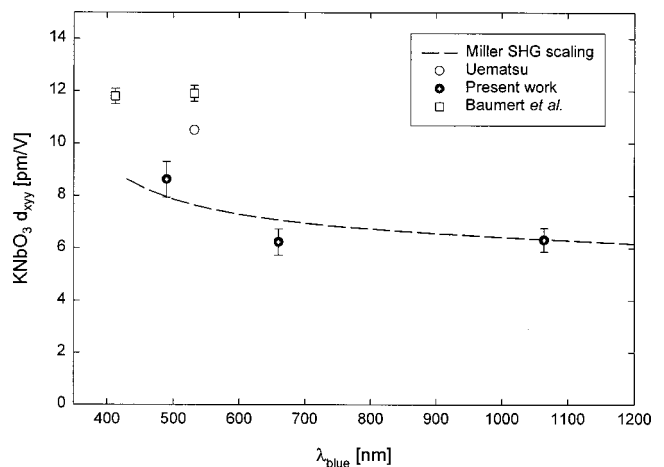


Fig. 8. KNbO₃ d_{xyy} value given by Roberts¹⁶ and measured in the present research. The dashed curve is Miller scaling normalized to the 532-nm point.

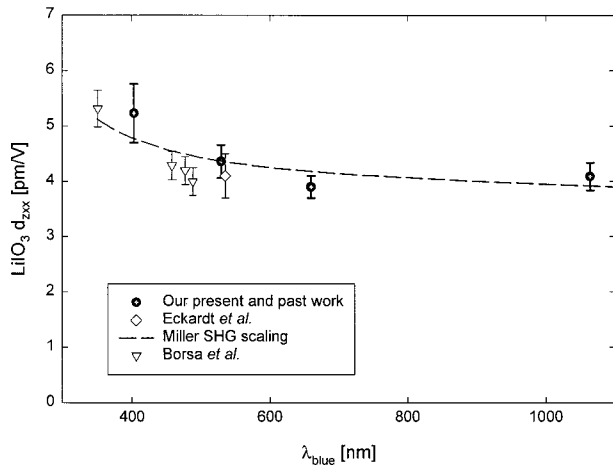


Fig. 9. LiIO_3 d_{zxx} values measured by Eckardt *et al.*²⁷ and us in the present and in previous research.¹⁵ Our 1064-nm point is derived by assuming $d_{zxx}/d_{yyy} = 0.49$, the value reported by Roberts¹⁶ at 532 nm. The dashed curve is Miller scaling normalized to our 532-nm point.

$\phi = 30^\circ$. From the measured gain we deduce $d_{\text{eff}} = 3.72 \pm 0.3$ pm/V and 3.79 ± 0.3 pm/V for the two crystals. For this process $d_{\text{eff}} = d_{zxx} \sin(\theta + \rho) - d_{yyy} \cos(\theta + \rho)$. Using the ratio (d_{yyy}/d_{zxx}) = -0.49 reported by Roberts¹⁶ for doubling 1064-nm light, we find $d_{zxx} = 3.49 \pm 0.28$ pm/V, as shown in Fig. 10. Frequency doubling of 1319 nm gave $d_{\text{eff}} = 4.05 \pm 0.3$ pm/V and $d_{zxx} = 3.77 \pm 0.3$ pm/V. The assumption of a constant ratio d_{yyy}/d_{zxx} independent of wavelength is not certain, but unless the ratio varies greatly over our wavelength range, our value of d_{zxx} would change little. We verified that the sign of this ratio is indeed negative for our samples by examining Maker fringes over a range of θ s for 1064-nm doubling.

Previous measurements of d_{zxx} by Eckardt *et al.*²⁷ and Shoji *et al.*¹ are included in Fig. 10. The measurements of Shoji *et al.* are based on parametric fluorescence of processes $488 \text{ nm} \rightarrow 678 \text{ nm} + 1741 \text{ nm}$ and $532 \text{ nm} \rightarrow 894 \text{ nm} + 1314 \text{ nm}$, on pulsed Maker-fringe second-harmonic generation (532 nm), on cw Maker-fringe second-harmonic generation of 1319-nm and 852-nm light, and on cw phase-matched difference-frequency mixing in 532 nm $- 1314 \text{ nm} \rightarrow 894 \text{ nm}$. We also plot a Miller-scaling curve adjusted to fit the data near 500 nm. Comparing our 1064-nm point with the Miller curve, it is clear that Miller scaling overestimates our 1064-nm d_{zxx} by only $\sim 10\%$. If we make a Miller adjustment to account for the nondegeneracy of the signal and the idler, this point would rise by 3.5%, bringing it within measurement error of the Miller curve.

G. BBO

Figure 11 summarizes measurements of d_{yyy} for BBO. For our parametric-gain process $532_e \text{ nm} \rightarrow 1550_o \text{ nm} + 810_e \text{ nm}$, $d_{\text{eff}} = d_{zxx} \sin(\theta + \rho) - d_{yyy} \cos(\theta + \rho)$. Using Shoji *et al.*'s²⁹ measured ratio for (d_{yyy}/d_{zxx}) of 55 for doubling 1064-nm light, our measured d_{eff} 's of 2.00 and 2.08 pm/V translate to $d_{yyy} = 2.23 \pm 0.18$ pm/V. We also measured d_{yyy} for frequency doubling of 1064 nm and 1319 nm. As seen in Table 1, the 1064-nm doubling mea-

surement agrees very well with the 532-nm-pumped parametric-gain measurement.

In other measurements, Shoji *et al.*²⁹ measured d_{yyy} using Maker-fringe second-harmonic measurements with cw lasers at wavelengths 532, 852, 1064, and 1313 nm. Eckardt *et al.*²⁷ measured it by phase-matched second-harmonic generation of a single-longitudinal-mode, Q-switched Nd:YAG laser at 1064 nm. Eimerl *et al.*³⁰ reported a value for doubling 1064-nm light but do not specify their measurement method. These are summarized in Fig. 11. Shoji *et al.*,²⁹ Eckardt *et al.*,²⁷ and we agree to well within measurement limits at 532 nm. The 266-nm and 426-nm values of Shoji *et al.* agree reasonably well with Miller scaling, while the 656-nm point falls below the curve. This is similar to their results for other crystals at this wavelength, although the deviation from the Miller curve is smaller here than in those reported earlier¹ for KTP, KNbO₃, and LiIO₃. Velsko *et al.*³¹ report $d_{yyy} = 2.23 \pm 0.16$ pm/V, measured by type I, phase-

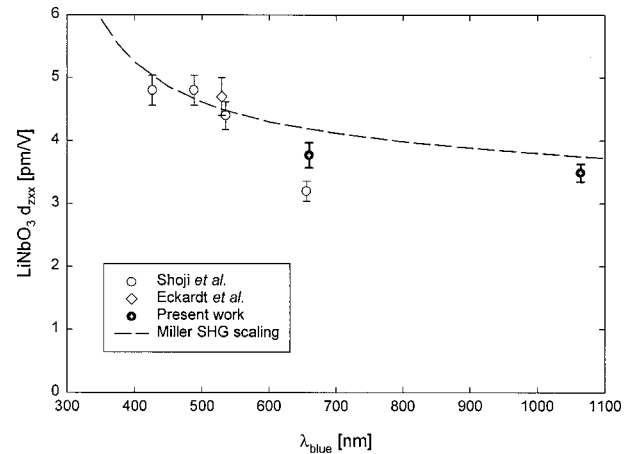


Fig. 10. LiNbO_3 d_{zxx} values measured by Shoji *et al.*,¹ Eckardt *et al.*,²⁷ and in the present research. The dashed curve is Miller scaling normalized to the best estimate 532-nm point.

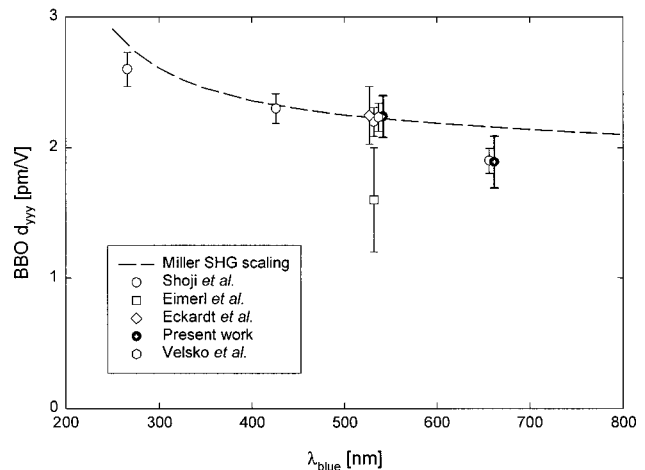


Fig. 11. BBO d_{yyy} values measured by Shoji *et al.*,¹ Eimerl *et al.*,³⁰ Eckardt *et al.*,²⁷ Velsko *et al.*,³¹ and in the present research. The dashed curve is Miller scaling normalized to the best-estimate 532-nm point. The points at 532 nm have been plotted with small wavelength offsets for clarity.

matched second-harmonic generation of 1064-nm light. Based on the limited data available, we conclude that Miller scaling is a reasonable approximation for d_{yyy} of BBO.

H. LBO

We measured $d_{yzz} = 1.04 \pm 0.08$ pm/V using 532_y nm $\rightarrow 1550_z$ nm + 810_z nm, in an x -cut crystal. Velsko *et al.*³¹ reported $d_{yzz} = 0.83 \pm 0.06$ pm/V, measured by type I, phase-matched second-harmonic generation of 1064-nm light in the x - y principal plane. Lin *et al.*³² also measured this coefficient, using Maker-fringe second-harmonic generation of 1079-nm light, and reported a value of 0.98 ± 0.2 pm/V. Not enough data exist at other wavelengths to reach a conclusion on the validity of Miller scaling for LBO.

4. CONCLUSIONS

The great majority of past measurements of nonlinear tensor elements, d_{ijk} , have been made by frequency doubling 1064-nm light. These values are often used at different wavelengths or are sometimes extrapolated to other wavelengths using Miller's scaling conjecture. We have extended the range of d_{ijk} measurements to longer wavelengths and have added new measurements in the visible range in an attempt to test Miller's hypothesis systematically for many common nonlinear crystals. For KDP, LiIO₃, LiNbO₃, and BBO, agreement with Miller scaling is good. Limited data for KTA suggest the coefficient d_{yyz} falls somewhat more rapidly with increasing wavelength than Miller scaling predicts. The data for KTP and KNbO₃ require some interpretation. For KTP we discussed some reasonable modifications or interpretations of previous measurements that, when combined with our new measurements, justify our conclusion that Miller scaling is a good approximation. Our KNbO₃ measurements taken alone match Miller scaling well, but our values disagree substantially with previous measurements. We find that in all cases the nonlinearity falls with increasing wavelength and there is no clear disagreement with Miller scaling, so we conclude that it provides an easily applied and reasonably accurate way to scale individual nonlinear coefficients with wavelength.

ACKNOWLEDGMENTS

This research was supported by the U.S. Department of Energy under contract DE-AC04-94AL85000. Sandia is a multiprogram laboratory operated by Sandia Corporation, a Lockheed Martin Company, for the U.S. Department of Energy.

REFERENCES

- I. Shoji, T. Kondo, A. Kitamoto, M. Shirane, and R. Ito, "Absolute scale of second-order nonlinear-optical coefficients," *J. Opt. Soc. Am. B* **14**, 2268–2294 (1997).
- B. Boulanger, J. P. Feve, G. Marnier, and B. Menaert, "Methodology for optical studies of nonlinear crystals: application to the isomorph family KTiOPO₄, KTiOAsO₄, RbTiOAsO₄, and CsTiOAsO₄," *Pure Appl. Opt.* **7**, 239–256 (1998).
- B. Boulanger, J. P. Feve, G. Marnier, B. Menaert, X. Cabriol, P. Villeval, and C. Bonnin, "Relative sign and absolute magnitude of $d^{(2)}$ nonlinear coefficients of KTP from second-harmonic-generation measurements," *J. Opt. Soc. Am. B* **11**, 750–757 (1994).
- B. Boulanger, J. P. Feve, G. Marnier, C. Bonnin, P. Villeval, and J. J. Zondy, "Absolute measurement of quadratic nonlinearities from phase-matched second-harmonic generation in a single KTP crystal cut as a sphere," *J. Opt. Soc. Am. B* **14**, 1380–1386 (1997).
- J.-J. Zondy, M. Abed, and A. Clairon, "Type-II frequency doubling at $\lambda=1.30$ μ m and $\lambda=2.53$ μ m in flux-grown potassium titanyl phosphate," *J. Opt. Soc. Am. B* **11**, 2004–2015 (1994).
- R. C. Miller, "Optical second harmonic generation in piezoelectric crystals," *Appl. Phys. Lett.* **5**, 17–19 (1964).
- R. W. Boyd, *Nonlinear Optics* (Academic, New York, 1992).
- C. G. B. Garrett and F. N. H. Robinson, "Miller's phenomenological rule for computing nonlinear susceptibilities," *IEEE J. Quantum Electron.* **QE-2**, 328–329 (1966).
- Y. R. Shen, *The Principles of Nonlinear Optics* (Wiley, New York, 1984).
- D. J. Armstrong, W. J. Alford, T. D. Raymond, and A. V. Smith, "Absolute measurement of the effective nonlinearities of KTP and BBO crystals by parametric amplification," *Appl. Opt.* **35**, 2032–2040 (1996).
- Function 2D-mix-LP within SNLO. The SNLO nonlinear optics code is available from A. V. Smith.
- H. Vanherzeele, J. D. Bierlein, and F. C. Zumsteg, "Index of refraction measurements and parametric generation in hydrothermally grown KTiOPO₄," *Appl. Opt.* **27**, 3314–3316 (1988).
- T. D. Raymond, W. J. Alford, M. H. Crawford, and A. A. Alberman, "Intracavity frequency doubling of a diode-pumped external-cavity surface-emitting semiconductor laser," *Opt. Lett.* **24**, 1127–1129 (1999).
- G. D. Boyd and D. A. Kleinman, "Parametric interaction of focused light beams," *J. Appl. Phys.* **39**, 3597–3639 (1968).
- R. J. Gehr and A. V. Smith, "Separated-beam nonphase-matched second-harmonic method of characterizing nonlinear optical crystals," *J. Opt. Soc. Am. B* **15**, 2298–2307 (1998).
- D. A. Roberts, "Simplified characterization of uniaxial and biaxial nonlinear optical crystals: a plea for standardization of nomenclature and conventions," *IEEE J. Quantum Electron.* **28**, 2057–2074 (1992).
- M. M. Choy and R. L. Byer, "Accurate second-order susceptibility measurements of visible and infrared nonlinear crystals," *Phys. Rev. B* **14**, 1693–1906 (1976).
- A. Anema and T. Rasing, "Relative signs of the nonlinear coefficients of potassium titanyl phosphate," *Appl. Opt.* **36**, 5902–5904 (1997).
- E. C. Cheung, K. Koch, G. T. Moore, and J. M. Liu, "Measurements of second-order nonlinear optical coefficients from the spectral brightness of parametric fluorescence," *Opt. Lett.* **19**, 168–170 (1994).
- T. Nishikawa and N. Uesugi, "Effects of walk-off and group velocity difference on the optical parametric generation in KTiOPO₄ crystals," *J. Appl. Phys.* **77**, 4941–4947 (1995).
- H. Vanherzeele and J. D. Bierlein, "Magnitude of the nonlinear-optical coefficients of KTiOPO₄," *Opt. Lett.* **17**, 982–984 (1992).
- L. K. Cheng, L. T. Cheng, J. Galperin, P. A. M. Hotsenpiller, and J. D. Bierlein, "Crystal growth and characterization of KTiOPO₄ isomorphs from the self-fluxes," *J. Cryst. Growth* **137**, 107–115 (1994).
- K. Kato, "Second-harmonic and sum-frequency generation in KTiOAsO₄," *IEEE J. Quantum Electron.* **30**, 881–883 (1994).
- Y. Uematsu, "Nonlinear optical properties of KNbO₃ single crystal in the orthorhombic phase," *Jpn. J. Appl. Phys.* **13**, 1362–1368 (1974).
- J.-C. Baumert, J. Hoffnagle, and P. Gunter, "Nonlinear optical effects in KNbO₃ crystals at Al_xGa_{1-x}As, dye, ruby

- and Nd:YAG laser wavelengths," *Proc. SPIE* **492**, 374–385 (1984).
26. R. Urschel, A. Fix, R. Wallenstein, D. Rytz, and B. Zysset, "Generation of tunable narrow-band midinfrared radiation in a type I potassium niobate optical parametric oscillator," *J. Opt. Soc. Am. B* **12**, 726–730 (1995).
 27. R. C. Eckardt, H. Masuda, Y. X. Fan, and R. L. Byer, "Absolute and relative nonlinear optical coefficients of KDP, KD*P, BaB₂O₄, LiIO₃, MgO:LiNbO₃, and KTP measured by phase-matched second-harmonic generation," *IEEE J. Quantum Electron.* **26**, 922–933 (1990).
 28. G. Borsa, S. Castelletto, A. Godone, C. Novero, and M. L. Rastello, "Measurement of second-order optical nonlinear coefficient from the absolute radiant power of parametric fluorescence in LiIO₃," *Opt. Rev.* **4**, 484–489 (1997).
 29. I. Shoji, H. Nakamura, K. Ohdaira, T. Kondo, R. Ito, T. Okamoto, K. Tatsuki, and S. Kubota, "Absolute measurement of second-order nonlinear-optical coefficients of β -BaB₂O₄ for visible to ultraviolet second-harmonic wavelengths," *J. Opt. Soc. Am. B* **16**, 620–624 (1999).
 30. D. Eimerl, L. Davis, S. Velsko, E. K. Graham, and A. Zalkin, "Optical, mechanical, and thermal properties of barium borate," *J. Appl. Phys.* **62**, 1968–1983 (1987).
 31. S. P. Velsko, M. Webb, L. Davis, and C. Huang, "Phase-matched harmonic generation in lithium triborate (LBO)," *IEEE J. Quantum Electron.* **27**, 2182–2192 (1991).
 32. S. Lin, Z. Sun, B. Wu, and C. Chen, "The nonlinear optical characteristics of a LiB₃O₅ crystal," *J. Appl. Phys.* **67**, 634–638 (1990).